STATISTICAL STUDY OF THE PRESSURE FLUCTUATIONS IN A FLUIDIZED BED

by

Rufino C. Lirag, Jr.* and Howard Littman
Rensselaer Polytechnic Institute
Troy, N. Y., 12181

Report : RPI - 3639 - 15

*now at: University of the Philippines
Diliman, Rizal, Philippines

DISCLAIMER

ABSTRACT

Pressure fluctuations in a fluidized bed and in the plenum below the bed were subjected to a statistical analysis to identify a periodic component in the fluctuations. The fluctuations observed are caused by fluctuations in the bed height resulting from bubbles escaping at the surface of the bed. The effect of gas velocity, bed height, particle size and density on the frequency and amplitude of the periodic component were investigated and the frequency used to calculate the average bubble size leaving the bed.

I. INTRODUCTION

Fluctuations of pressure and pressure drop have been observed in gas fluidized beds by many investigators. Tamarin (17) and Hiby (6) have suggested that these fluctuations are associated with the escape of bubbles from the surface of the bed. Kang, Sutherland and Osberg (8) on the other hand did not find a correlation between pressure drop fluctuations in the bed and bed height fluctuations, and attributed pressure fluctuations to the action of bubbles which cause changes in gas flow and porosity in the dense phase.

Most investigators (5, 14, 16, 18) however, have used the fluctuations to determine indices of fluidization quality which are interpreted as measures of the bubble size.* Although the frequencies of fluctuation were determined in a somewhat subjective manner, they are of the right order of magnitude.

Sutherland (15) and Kang et al (8) have both recorded pressure drop fluctuations between two different locations in the bed. The latter investigators calculated the probability density function, root mean square and power spectral density of the fluctuations but did not relate these quantitatively to the bubble size.

Periodic pressure fluctuations both at the top and bottom of shallow beds ($L/D_p < 10$) have been noted by Hiby (6)

---

* Other investigators have used density fluctuations to the same end (2, 3, 12, 18).

and he has explained them in terms of the vertical oscillation of a single particle around its equilibrium position. Applying the equation of motion for a harmonic oscillator to a single particle with a restoring force given by the sum of its weight and lifting force exerted by the gas flow*, Hiby calculates the natural frequency of oscillation in short beds. In deeper beds, Hiby suggests the vertical oscillations persist in the first ten particle diameters of the bed; above that level, the oscillations are disrupted causing periodic formation of bubbles.

Jones and Pyle (7) also consider the behavior of a single particle under a restoring force to calculate the frequency of oscillation of the bed. Their restoring force is given by the sum of the particle weight, a non-linear drag term and a viscous damping term resulting from the dilitation of adjacent particles. A periodic driving force is derived from the supporting oscillating gas stream. They find that damping due to viscous stresses becomes important in reducing the oscillation frequency as the particle size is reduced and that the onset of bubbling in response to an increase in the fluidizing velocity results from increasing amplitude of oscillation or decreasing damping coefficient.

The frequency of fluctuation varies with bed height in a manner which depends on the rate of bubble coalescence. Thus bubble initiation and growth after initiation determine the

---

* Hiby uses Ergun's equation (4) which applies to a packed bed of particles to calculate the lifting force.

bubble size leaving the surface of the bed. The first step is very dependent on the distributor and the bubble initiation mechanism in the bed, and the latter on the bed itself.

In this paper, pressure fluctuations in the bed and plenum are subjected to a statistical analysis to clearly identify a periodic component in the fluctuations and the cause of the fluctuations. The effect of bed parameters on the fluctuation frequency are determined and bubble sizes are calculated from the frequency.

II. EQUIPMENT AND PROCEDURE

Equipment - A schematic diagram of the entire laboratory apparatus is shown in Figure 1. It consists of a column and flow system, a pressure probe and transducer, and amplifying and recording equipment.

Air was used as the fluidizing fluid and the solid particles were copper and glass beads in the size range 132 to 500 microns. Particle properties are given in Table 1.

The column (Figure 2) is a Plexiglas cylinder 2-1/2 inches in diameter and 24 inches long. A series of pressure taps 2 inches apart vertically are located in the column wall for detection of the pressure signals at several locations above the distributor plate. The probe assembly is made such that its radial position in the bed can be changed.

A sintered stainless steel disc of 20 micron porosity was used as a distributor plate. A second plate (porosity: 165 microns) was used with a one-inch high spacer to form a plenum below the bed. An O-ring sealed the space between the inner wall of the column and the plates.

The pressure probe was made of 1/4-inch O.D. copper tubing, one end of which was covered with a screen to prevent the solid particles from entering the probe; the other end was connected to the pressure transducer. Two transducers were used in this work -- a Baratron model 77H capacitance type pressure sensor and a Statham model PM5TC unbonded strain gage transducer. The natural frequency of the Statham is 200 Hertz and the frequency response is flat up to about 40 Hertz. Such a response is adequate in this work since the maximum frequency encountered was only 25 Hertz.
The Baratron and Statham transducers gave indentical traces when inserted into the bed at the same location. The range of the Statham transducer is 0 to 0.15 psi.

The Baratron pressure meter consists of two components: a type 77-H-30 pressure sensor* and a type 77-M-XRP-2 indicator. The head is essentially made of a thin stainless steel diaphragm which has been highly stretched to mirror-like flatness. The diaphragm forms a capacitor with each of the two nickel electrodes situated above and below the diaphragm. The electrodes are insulated from the diaphragm by ceramic discs which are sandwiched between the diaphragm and each electrode. This whole assembly is then held together by a high force clamp which extends around the periphery of the head.

Changes in pressure on one side of the diaphragm cause and AC bridge circuit to become unbalanced producing a voltage

---

* MKS Baratron Pressure Meter, MKS Instruments, Burlington, Mass.

output in the detector circuit. For steady state measurements, the bridge is rebalanced by means of a multitap ratio transformer incorporated in the bridge circuit. The transformer tap is adjusted by three decade switches and an interpolating potentiometer decade. The switch dials are directly calibrated in mm. Hg and may be read directly to an accuracy of 0.001 mm. Hg.

This circuit was also used to buck out the mean (or a steady component close to the mean) of the fluctuating pressure signals obtained in the bed and plenum whenever its magnitude was within the range of the Baratron (30 mm. Hg.). When this was not the case, the reference side of the pressure head was connected to the same signal source and the mean of the pressure signal on the reference side removed by a suitable length of small copper tubing connected to an air tank.

The millivolt-level pressure signals were amplified up to 1000 times using a Hewlett-Packard Model 2470A data amplifier, and the output recorded as a pressure-time curve on a Honeywell Model 906-C Visicorder. The signals to be recorded were visually inspected on an oscilloscope before recording.

Procedure - The pressure sensor is attached to one of the pressure taps in the wall of the column (located at different distances above the distributor plate). A known weight of the solid particles is added to the column and the air flow rate through the bed increased until fluidization occurs. The air flow is then shut off and the static height of the bed (L_s) measured.

A run is made by obtaining a pressure-time record for a fixed value of all the fluidized bed variables (probe location,

particle size and density, static bed height, and gas flow rate). Before recording the pressure fluctuations, the signal is observed on the oscilloscope and the time lines set according to the apparent frequency of the fluctuations. The time lines on the Visicorder are set by means of an external pulse generator.

The pressure-time record was digitized manually.

III. CALCULATIONS

The statistical properties of the pressure signals calculated are the mean, root mean square, probability density, autocorrelation, cross-correlation and the power spectral density functions. Details of the calculations are given by Lirag (11).

For each experimental run, there are two parameters which may be varied depending on the type signal expected, namely, the sampling interval and the record length. If the Nyquist frequency is assumed known* and equal to y_c, the sampling intervals should be $h = 1/2y_c$ so that aliasing may be avoided.

It is always desirable to use a long record to improve the accuracy of the calculations (particularly the power spectral density). Since this increases the labor and cost of the calculations, a compromise was made and a record length of about one minute was used in all runs. Subsequent calculation of the statistical error** in the estimate of the spectrum showed that

---

* This frequency can be estimated from the time between peaks on the pressure-time recorded (see Figure 3).

** Normalized Standard Error = $\left[\frac{E\{(\hat{\Phi} - \Phi)^2\}}{\Phi^2}\right]^{1/2}$

in all runs the error always remained less than 23%. The error in the estimation of the other properties are considerably smaller.

IV. RESULTS AND DISCUSSION

Pressure signals in the plenum and in the bed were obtained for different values of the bed height, particle size, particle density, and gas flow rate. They were analyzed statistically in order to find a relation between the statistical parameters calculated from the fluctuations and the characteristics of the bed.

A. The Periodic Component of the Pressure Fluctuations

Representative samples of the pressure fluctuations obtained are shown in Figures 3 and 4. As first reported by Hiby, the fluctuations are sinusoidal in shallow beds. In deeper beds, they are irregular with peaks of varying height (Figure 3). A close visual observation of the traces reveals some regular patterns. Pressure peaks are regularly spaced (Figure 3) and the pressure generally decreases quite steeply after passing a peak. The fluctuations in the bed and plenum were analyzed by calculating their mean, variance, probability density, autocorrelation and power spectral density functions. Of these statistical parameters only the probability density, autocorrrelation and power spectral density are relevant for identifying a periodic component in the fluctuations.*

The probability density function for a typical bed

---

* For sinusoidal pressure fluctuations, calculation of the statistical parameters are obviously unnecessary.

whose pressure fluctuation pattern is similar to that shown in Figure 3 always shows a hump near the mean value of the signal (Figure 5) indicating the presence of a periodic component. The corresponding autocorrelation function (Figure 6) exhibits the characteristic trends of both random and periodic signals. A maximum is obtained at zero time lag and the function becomes sinusoidal with a fairly constant period as the time lag is increased. This character of the autocorrelograms for both copper and glass particle beds proves the presence of a periodic component in the pressure fluctuations of both the bed and the plenum. The amplitude of the periodic component is smaller in the bed than in the plenum.

The most obvious and perhaps the most important feature of the power spectral density obtained in all runs is the presence of a sharp peak (Figure 7). The location, size and width* of the peak obtained depends on the bed parameters.

The concentration of the power of the signal into a very narrow frequency band, with a width of less than one cycle per second, confirms the presence of a periodic component in the pressure signals. The same frequency is always obtained from the power spectrum and the autocorrelation functions as shown in Table 2 for a few representative runs. The probability density, auto-correlation and power spectral density functions are all consistent with one another and clearly demonstrate the presence of a periodic component in the fluctuations.

---

* The width of the peak is taken at one-half the peak height.

B. The Cause of Pressure Fluctuations

The shape of the pressure readings in the plenum and those in the bed are similar (Figures 3 and 4). A pressure increase in the bed is followed by a corresponding increase in the plenum with a time lag less than one sixtieth of a second. The cross-correlation function for the bed and plenum signals confirms this short time lag. In Figure 3, the separation between the two probes is 4.5 inches and assuming the time lag is as much as one sixtieth of a second, the propagation velocity of the pressure wave is 270 inches/sec (686 cm/sec). This is much higher than the phase velocity associated with waves obtained from linearized stability analyses of the equations of motion.

Typical of the results obtained from stability analyses is the theory of Anderson and Jackson (1). In that theory a perturbation in the state of uniform fluidization causes a plane wave pressure disturbance which grows in amplitude as it travels upward through the bed. Presumably such disturbances are initiated near the distributor plate and are responsible for the initiation of bubbles in the bed. Since the theoretical phase velocity given in Table 3 is so much lower than the experimental value, the theory cannot possibly describe the cause of the fluctuations observed. Propagation velocities of the magnitude observed are possible if the fluctuations are related to bed height fluctuations caused by the escape of bubbles from the surface of the bed as suggested by Tamarin (17) and Hiby (6).

The effect of bed height on the frequency of the pressure fluctuations in the plenum (Figure 8) strongly indicates that the signals are initiated at the top of the bed and transmitted downward. The frequency in the plenum if caused by bubbles originating near the distributor plate should be unaffected by bed length. If on the other hand, the frequency is related to bed height fluctuations, it should decrease with bed height because of bubble coalescence. Figure 8 clearly shows the latter hypothesis is correct.

C. The Frequency and Amplitude of the Periodic Component of the Fluctuations.

Bubbles undoubtedly result from fluid mechanical instabilities in the bed near the distributor plate so that the frequency of fluctuation calculated from the stability analysis should predict the frequency at which bubbles are initiated in the bed. Furthermore, the experimental frequencies, should be comparable to the initiation frequency for low values of L_s/D_p and U/U_o. This comparison, shown in Table 3, is excellent if the bed viscosity ($\lambda_o^s + 4/3\ \mu_o^s$) is taken as slightly greater than 8 poise for the 500μ glass particles and slightly greater than 4 poise for the 132μ copper particles. Such viscosities are quite reasonable.

The bed height has a significant effect on the fluctuation frequency as seen in Figure 8. The frequency decreases as the bed height increases because of bubble

coalescence and the increase in amplitude expected as a result of coalescence can be seen in Figure 11*. The frequency also decreases with increasing particle size in the shorter beds. Since the curves for 500μ and 318μ glass particles cross at the higher bed heights used, bubble coalescence per unit of bed length appears to increase as the particle size is lowered. Such an effect is consistent with the results obtained for the 132μ copper particles.

Figure 9 shows the frequency as a function of the bed height in particle diameters. Raising L_s/D_p always lowers the frequency. For the 132μ copper particles, the frequency is proportional to $(L_s/D_p)^{-1}$. For glass particles, the frequency decreases slightly with L_s/D_p in shallow beds but in deeper beds the effect is similar to that for the copper particles. Hiby's results for glass particles in shallow beds are shown on this plot and they agree well with the data obtained in this study. The natural frequency of oscillation calculated by Jones and Pyle (applicable to shallow beds) also agrees with the data in Figure 9.

The frequency increases slightly with U/U_o except in the shallow beds of 500μ glass particles. The result rather clearly shows that when the gas velocity is increased above the minimum in a bed of given height, the excess air goes primarily into producing larger bubbles. The increase in

* Figure 13 shows how the amplitude decreases with distance from the top of the bed in a particular bed at a particular gas velocity. Equations are given in Table 4.

amplitude expected is seen in Figure 13.

Hiby's theory predicts that the frequency should decrease with increased velocity but found no effect of U/U_o experimentally. Jones and Pyle predicted and found the frequency to increase with U/U_o to the undamped natural frequency of the system. For glass particles, the frequency increased with U/U_o in the range of 1 to about 2, the effect being most pronounced for the smaller sizes (150μ and larger). For 500μ particles, they found no effect of U/U_o.

There seems to be both theoretical and experimental variation in the results of the various investigators. The reasons for this are not clear.

Figures 5, 6 and 7 show that the amplitude of the periodic component is lower in the plenum than in the bed and Figure 13 shows that this amplitude increases exponentially with distance from the distributor plate. The experimental growth distance* is lower than, but of the same order of magnitude, as that predicted by Anderson and Jackson (Tables 3 and 4).

The amplitude of the periodic component of the fluctuations is related to the size of bubbles escaping from the bed. The amplitude in the plenum increases approximately as the square of the gas velocity ratio, U/U_o (Figure 11) and for a fixed value of U/U_o, the amplitude increases with bed height, particle size and particle density. Figure 12 shows

* The growth distance is defined as the distance of travel in which the amplitude grows by a factor of e. In this work, the wave is being attenuated as it goes down the column.

that the amplitude increases with bed height to the 1.3 power. For a fixed bed height, the amplitude increases with particle size, particle density and U/U_o. These results suggest that the average bubble size at the top of the bed increases with bed height, flow rate, particle size and particle density.

D. The Average Size of the Bubbles Escaping the Bed

The performance and characteristics of fluidized beds are largely determined by the average size and frequency of the bubbles passing through it. These two bubble properties are simply related if the two-phase theory is assumed valid.

In this section, the average size of the bubbles escaping from the bed are determined from the excess flow above the minimum and the frequency of the pressure fluctuations in the plenum. The results are then compared with existing correlations in the literature.

The following assumptions were made in order to calculate the average size of the bubbles at the top of the bed:

1. The two-phase theory was assumed valid and used to calculate the volume of gas that flows through the bed as bubbles.
2. The dominant frequency (frequency of the peak in the power spectrum) was taken equal to the bubble frequency at the top of the bed.
3. The bubble size calculation is valid only when there is one bubble at a time escaping the surface of the bed. Otherwise, the calculation

gives only the equivalent diameter of those bubbles that escape simultaneously taken as one single (obviously bigger) bubble. Bubble sizes were not calculated from the shallow bed runs because it was observed that more than one bubble escaped the bed simultaneously.

With these assumptions, the average bubble size (equivalent sphere*) is:

$$\overline{D}_B = (6/\pi)^{1/3} \left(\frac{Q-Q_o}{y_B} \right)^{1/3} \qquad (1)$$

Results are given in Table 6 for bubbling beds only.

The validity of the two phase theory has received considerable attention in the past few years. Evidence, both theoretical and experimental, has been accumulating which seriously challenges that theory (6a). Where the gas flow through the bubble and the reduced cross-sectional area of the dense phase at any level due to bubbles are taken into account, the visible bubble flow is less than that predicted from the two phase theory. With these assumptions plus the one that the flow through the dense phase is at the minimum fluidizing velocity, the average bubble size is:

$$\overline{D}_B = \left(\frac{6}{\pi} \right)^{1/3} \left[\frac{(Q-Q_o) - (m-1)\epsilon_b Q_o}{y_B} \right]^{1/3} \qquad (2)$$

---

*To calculate the average frontal diameter of the bubbles multiply $\overline{D}_B$ by 1.10.

Since there is no generally acceptable method for calculating m and ϵ_b, equation (1) is commonly used to calculate $\overline{D}_B$ and represents the maximum bubble size. It is a reasonable estimate of the actual bubble size particularly when the ratio of the bubble to minimum fluidizing velocity is above 5 (10).

There are two correlations for the bubble size currently available in the literature. They are:

Kato and Wen (9)

$$\overline{D}_B = \frac{\frac{6}{\pi}\left[\left(\frac{U-U_o}{n}\right)\right]^{0.4}}{g^{0.2}} + 1.4\, D_p \rho_p L \frac{U}{U_o} \qquad \text{(cgs. units)} \qquad (3)$$

Park et al* (13)

$$\overline{D}_B = 4.33\, D_p^{1.5}\, L \left[\frac{U-U_o}{U_o}\right]^{0.77} \qquad \text{(Units: cm. and sec.)} \qquad (4)$$

Table 6 compares the average bubble sizes calculated from the fluctuation data using equation (1) with that calculated from Kato and Wen correlation. The comparison (Figure 14) is remarkably good considering the state of the art. The scatter is within that of the data used by Kato and Wen to obtain their correlation.

Bubble sizes calculated from equation (4) for the runs in Table 6 gives bubble sizes which are much too small.

---

*Park et al use, $\overline{\ell}$, the average bubble length in their correlation. $\overline{D}_B = 1.30\overline{\ell}$

Two equations are available for calculating the bubble size from the frequency. Tamarin's equation is

$$\bar{D}_B = 18.31 \frac{D_p^{\frac{1}{2}}}{y_B} \left[\frac{U}{U_o} - 1\right]^{0.275} \qquad \text{(units: cm. and sec.)} \qquad (5)$$

Using the experimental frequency of the periodic component, Tamarin's bubble size is always smaller than that obtained from equation (1). For example, consider run 54 in which the glass particle diameter is 318 μ, $U/U_o = 1.23$ and $y_B = 2.90$ Hz. $\bar{D}_B$ calculated from equation (5) is 1.28 cm., while $\bar{D}_B$ experimental (Table 6) is 3.20 cm.

The equation given by Kunii and Levenspiel (10) is

$$\bar{D}_B = \frac{1.5}{f_B} (U - U_o) \qquad \text{(units: cm. and sec.)} \qquad (6)$$

f_B is the point bubble frequency which differs from the bubble frequency passing through a horizontal plane, y_B as pointed out by Geldart (6a). The bubbles given in Table 6 are all greater than half the column diameter and for such sizes y_B and f_B can be assumed equal.

$\bar{D}_B$ calculated from equation 6 for run 54 is 0.84 cm. The result though much lower than the 3.20 cm value in Table 6 is not unexpected since Geldart (6b) has shown that the coefficient 1.5 is much too low when the bubble flow rate is low.

Prediction of the bubble size in a fluidized bed is still an open question and considerably more work is needed in the area. The frequency of the periodic component of the fluctuations

is easy to obtain and useful for calculating bubble sizes where one bubble escapes at a time from the bed surface. The frequency of the periodic component could also be a useful way of monitoring changes in bed conditions in operating fluidized beds and for studying slugging phenomena.

V. CONCLUSIONS

1. The probability density, autocorrelation and power spectral density functions of the pressure fluctuations are all consistent with one another and clearly demonstrate the presence of a periodic component in the fluctuations.
2. The pressure fluctuations observed are caused by bed height fluctuations resulting from bubbles escaping the surface of the bed.
3. The frequency of the periodic component is generally lowered by raising the bed height and increasing the particle size. The gas velocity ratio, U/U_o, has little effect on the frequency.
4. The average bubble size calculated using the plenum frequency agrees quite well with the bubble size correlation of Kato and Wen (9).
5. The amplitude of the periodic component increases with bed height, particle size, particle density, and the gas velocity ratio, U/U_o.

REFERENCES

1. Anderson, T. B., Jackson, Roy, "Fluid Mechanical Description of Fluidized Beds, Stability of the State of Uniform Fluidization", Ind. Eng. Chem. Fundamentals 7 (1), 12-21 (1968).

2. Bailie, R.C., Fan, L., Stewart, Jr., "Uniformity and Stability of Fluidized Beds", Ind. Eng. Chem. 53 (7), 567-569 (1961).

3. Dotson, J., "Factors Affecting Density Transients in a Fluidized Bed", A.I.Ch.E.J. 5 (2), 169-174 (1959).

4. Ergun, S., Chem. Eng. Progr. 48 89 (1952).

5. Fiocco, R.J., Staffin, H.K., "Pressure Patterns of Fluidized Beds", paper presented at A.I.Ch.E. Houston Meeting (1967).

6. Hiby, J. W., "Periodic Phenomena Connected with Gas-Solid Fluidization", Proceedings of the International Symposium on Fluidization, Eindhoven, p.99, Netherlands University Press, Amsterdam (1967).

6a. Geldart, D., "The Size and Frequency of Bubbles in Two and Three Dimensional Gas Fluidized Beds," Powder Technol. 4, 41-55 (1970/71)

6b. Geldart, D., "The Expansion of Bubbling Fluidized Beds", Powder Technol. 1 355-368 (1968).

7. Jones, B.R.E., Pyle, D.L., Chem. Eng. Progr. Symp. Ser.

8. Kang, W.K., Sutherland, J.P., Osberg, G.L., "Pressure Fluctuations in a Fluidized Bed With and Without Screen Cylindrical Packings", Ind. Eng. Chem. Fundamentals 6 (4), 449-504 (1967).

9. Kato, K., Wen, C.Y., "Bubble Assemblage Model for Fluidized Bed Catalytic Reactors", Chem. Eng. Sci. 24 (8), 1351-1369 (1969).

10. Kunii, D., Levenspiel, O., Fluidization Engineering, John Wiley, New York (1969).

11. Lirag, R.C., Jr., "Statistical Study of Pressure Fluctuations in a Fluidized Bed", Rensselaer Polytechnic Institute, Troy, New York (1970).

12. Morse, R.D., Ballou, C.O., "The Uniformity of Fluidization - Its Measurement and Use", Chem. Eng. Prog. 47 (4), 199-204 (1951).

13. Park, W.H., Kang, W.K., Capes,C.E., Osberg, G.L., "The Properties of Bubbles in Fluidized Beds of Conducting Particles as Measured by an Electroresistivity Probe", Chem. Eng. Sci. 24 (5) 851-865 (1969).

14. Shuster, W., Kisliak, P.,"The Measurement of Fluidization Quality", Chem. Eng. Prog. 48 (9), 455-458 (1952).

15. Sutherland, K. S., "The Effect of Particle Size on the Properties of Gas Fluidized Beds", U. S. Atomic Energy Commission Report, ANL-6907, July 1964.

16. Swinehart, Frederick Melvin, "A Statistical Study of Local Wall Pressure Fluctuations in Gas Fluidized Columns", Ph.D. Dissertation, The University of Michigan, Ann Arbor (1966).

17. Tamarin, A. I., "The Origin of Self-Excited Oscillations in Fluidized Beds", Intern. Chem. Eng. 4 (1), 50-54 (1964).

18. Winter, O., "Density and Pressure Fluctuations in Gas Fluidized Beds", A.I.Ch.E. Journal, 14 (3), 426-34 (1968).

NOMENCLATURE

$\overline{D}_B$ = Average bubble diameter escaping the bed (equivalent sphere)

$E\{\ \}$ = Expectation of $\{\ \}$

g = Gravitational acceleration

$\overline{\ell}$ = Average bubble length, reference 13.

L = Distance above distributor plate

L_o = Height of the bed surface above the distributor plate at incipient fluidization

L_s = Static bed height

m = A dimensionless measure of gas through flow in a bubble, see reference 6a

n = Number of holes per unit area of distributor taken as $0.1/cm^2$

$\overline{P}$ = Amplitude of the periodic component

$\overline{P}_g$ = Mean pressure of the pressure fluctuation

Q = Volumetric flow rate

Q_o = Volumetric flow rate at minimum fluidization

RMS = Root mean square of the signals

U = Superficial gas velocity

U_o = Superficial gas velocity at minimum fluidization

y_B = Bubble frequency at a horizontal plane in the bed

Greek Notations

ϵ_b = Fraction of bed cross-section occupied by bubbles, see reference 6a

μ = Microns

ρ_p = Particle density

Φ = Arbitrary statistical parameter

$\hat{\Phi}$ = Estimate of Φ

TABLE 1

Physical Properties of the Solid Particles

Material	Approximate Shape	Density (gm./cc.)	Minimum Fluidizing Velocity (cm/sec)	Particle Diameter (microns)
Glass	spherical	2.42	19.1	500
Glass	spherical	2.48	7.09	318
Glass	spherical	2.43	3.65	218
Copper	spherical	7.72	4.85	132

TABLE 2

Comparison of the Frequency of the Periodic Component Using the Power Spectrum and the Auto-correlation Functions

Run Number	Frequency using autocorrelogram (Hz)	Frequency of peak in spectrum (Hz)
3	5.75	5.80
4	5.56	5.80
13	2.28	2.56
14	2.38	2.56
34	2.78	2.60
35	2.78	2.60
47	0.633	0.70
80	2.48	2.30

TABLE 3

Propagation Characteristics of
500μ Glass Particles

$\lambda_o^s + 4/3\mu_o^s$ (Poise)	Wave Number, k_x, (1/cm) cm^{-1}	Growth Distance Δx (cm)	Phase Velocity, V_p, (cm/sec)	Dominant Frequency, $\frac{V_p k_x}{2\pi}$ (Hz.)
4	10.5	41.6	11.4	19
8	4.5	20.1	15.8	11.3
16	3.0	17.4	17.1	8.16
24	2.5	17.2	17.1	6.8

Propagation Characteristics of
132μ Copper Particles

4	20.5	46.4	10.5	34.2
8	9.5	28.5	13.0	19.7
16	6.5	24.5	14.4	14.9
24	5.5	15.4	14.6	12.8

Experimental Frequencies in Shallow Beds (This work)

Material	$\frac{L_s}{D_p}$	$\frac{U}{U_o}$	Dominant Frequency (Hz)
500μ glass	14.2	1.23	10.64
132μ copper	38.5	1.23	12.65

Calculated from the theory of Anderson and Jackson (1)

TABLE 4

Variation of the Amplitude of the Periodic Component of the Pressure Fluctuations with Distance from the Distributor Plate

$\overline{P} = Ae^{Bx}$ where $\overline{P}$ is in mm. Hg and x in cm.

Material	Particle Size microns	U/U_o	A mm.Hg.	B cm^{-1}	Growth Distance (cm)
Glass	500	1.23	0.39	0.0772	12.95
Glass	500	1.60	0.74	0.0875	11.43
Glass	500	1.97	1.85	0.0679	14.73
Copper	132	1.21	0.31	0.0729	13.71

Table 5

Frequency and Amplitude of Periodic Component of Pressure Fluctuations

Run No.	L_s (in)	L_o (in)	Q (ft^3/min)	$\frac{U}{U_o}$	Probe Loc. (in above dist.)	Freq. of Peak in Spectrum (Hz)	Amplitude of Periodic Comp. (mm.Hg)
				500 Micron Glass Particles			
1	0.28	0.30	1.57	1.23	Plenum	10.64	0.062
2	0.28	0.30	1.80	1.40	Plenum	10.64	0.093
3	0.28	0.30	2.04	1.60	Plenum	10.42	0.128
4	0.28	0.30	2.28	1.78	Plenum	11.87	0.120
5	0.60	0.62	1.57	1.23	Plenum	7.87	0.146
6	0.60	0.62	2.04	1.60	Plenum	9.64	0.193
7	0.60	0.62	2.52	1.97	Plenum	9.67	0.179
8	1.75	1.80	1.57	1.23	Plenum	5.65	0.073
9	1.75	1.80	2.04	1.60	Plenum	6.05	0.126
10	1.75	1.80	2.04	1.60	0.5	6.05	0.155
11	1.75	1.80	2.75	2.15	Plenum	5.80	0.349
12	1.75	1.80	2.75	2.15	0.5	5.80	0.402
13	1.75	1.80	3.47	2.70	Plenum	6.30	0.390
14	1.75	1.80	3.47	2.70	0.5	6.30	0.526
15	1.75	1.80	4.06	3.17	Plenum	6.65	0.512
16	1.75	1.80	4.06	3.17	0.5	6.65	0.583
17	4.1	4.15	1.57	1.23	Plenum	3.75	0.127
18	6.1	6.20	1.57	1.23	Plenum	2.8	0.166
19	8.5	8.65	1.45	1.13	0.5	2.60	0.256
20	8.5	8.65	1.45	1.13	6.5	2.60	0.256
21	8.5	8.65	1.57	1.23	Plenum	2.56	0.379
22	8.5	8.65	1.57	1.23	0.5	2.55	0.410
23	8.5	8.65	1.57	1.23	2.5		
24	8.5	8.65	1.57	1.23	4.5	2.56	0.950
25	8.5	8.65	1.57	1.23	6.5	2.55	1.31
26	8.5	8.65	1.80	1.40	Plenum	2.45	0.440
29	8.5	8.65	2.04	1.60	Plenum	2.80	0.985
30	8.5	8.65	2.04	1.60	0.5	2.40	0.850

Run No.	L_s (in)	L_o (in)	Q (ft^3/min)	$\frac{U}{U_o}$	Probe Loc. (in above dist.)	Freq. of Peak in Spectrum (Hz)	Amplitude of Periodic Comp. (mm.Hg)
31	8.5	8.65	2.04	1.60	2.5		
32	8.5	8.65	2.04	1.60	4.5	2.80	2.04
33	8.5	8.65	2.04	1.60	6.5	2.40	3.42
34	8.5	8.65	2.28	1.78	Plenum	2.75	1.23
38	8.5	8.65	2.52	1.97	Plenum	2.78	1.80
39	8.5	8.65	2.52	1.97	0.5	2.15	2.00
41	8.5	8.65	2.52	1.97	4.5	2.78	3.25
42	8.5	8.65	2.52	1.97	6.5	2.15	5.65
43	8.5	8.65	2.75	2.15	Plenum	2.95	2.15
45	11.0	11.2	1.57	1.23	Plenum	1.82	0.497
46	11.0	11.2	1.57	1.23	6.5	1.80	1.45
47	12.6	12.85	1.57	1.23	Plenum	1.25	0.600
48	12.6	12.85	1.57	1.23	6.5	1.25	1.62
49	12.6	12.85	2.04	1.60	Plenum	2.10	1.10
50	12.6	12.85	2.04	1.60	6.5	2.10	5.88
					318 Micron Glass Particles		
51	0.57	0.60	0.583	1.23	Plenum	14.0	0.005
52	1.45	1.50	0.583	1.23	Plenum	9.4	0.0079
53	3.25	3.30	0.583	1.23	Plenum	5.5	0.0241
54	6.45	6.55	0.583	1.23	Plenum	2.9	0.0714
55	8.40	8.55	0.583	1.23	Plenum	2.3	0.158
56	8.40	8.55	0.583	1.23	4.5	2.3	0.276
					218 Micron Glass Particles		
57	8.25	8.45	0.302	1.23	Plenum	1.2	0.0715
58	8.25	8.45	0.302	1.23	4.5	1.47	0.100
60	8.25	8.45	0.430	1.70	Plenum	1.18	0.100
61	8.25	8.45	0.430	1.70	4.5	2.35	0.120
63	8.25	8.45	0.563	2.3	Plenum	1.60	0.255
64	8.25	8.45	0.947	3.9	Plenum	1.70	0.915
65	8.25	8.45	0.947	3.9	4.5	2.05	1.16

Run No.	L_s (in)	L_o (in)	Q (ft^3/min)	$\frac{U}{U_o}$	Probe Loc. (in above dist.)	Freq. of Peak in Spectrum (Hz)	Amplitude of Periodic Comp. (mm Hg)
			132 Micron Copper Particles				
67	0.2	0.2	0.394	1.21	Plenum	27.5	0.00235
68	0.5	0.52	0.394	1.21	Plenum	12.65	0.018
69	1.1	1.15	0.394	1.21	Plenum	4.15	0.048
70	4.1	4.15	0.394	1.21	Plenum	1.35	0.134
71	6.05	6.15	0.394	1.21	Plenum	0.85	0.195
75	8.15	8.25	0.394	1.21	Plenum	0.7	0.308
-	8.15	8.25	0.394	1.21	0.5	0.7	0.325
-	8.15	8.25	0.394	1.21	2.5	0.8	0.51
76	8.15	8.25	0.394	1.21	4.5	-	0.51
-	8.15	8.25	0.394	1.21	6.5	0.48	1.04
77	8.15	8.25	0.521	1.60	Plenum	0.90	0.470
78	8.15	8.25	0.586	1.80	Plenum	0.95	0.590
79	8.15	8.25	0.852	2.60	Plenum	1.30	0.960
80	8.15	8.25	0.950	2.90	Plenum	1.40	1.06
81	8.15	8.25	0.950	2.90	4.5	1.55	2.35
82	10.6	10.9	0.394	1.21	Plenum	0.41	0.584
83	10.6	10.9	0.394	1.21	4.5	0.60	0.645
84	10.6	10.9	0.852	2.60	Plenum	1.10	2.92
85	10.6	10.9	0.852	2.60	4.5	1.35	3.22

TABLE 6

Average Bubble Size in Bubbling Beds

Run Number	$\overline{D}_b$ (this work) cm	$\overline{D}_b$ (Kato and Wen) cm
17	4.14	3.68
18	4.56	4.76
21	4.70	6.06
26	5.74	7.52
45	5.27	7.41
54	3.24	3.25
55	3.50	3.95
60	5.08	3.90
63	5.64	5.19
70	3.57	2.64
71	4.17	3.52
75	4.45	4.43
77	5.80	6.04
78	5.32	6.79
82	5.32	5.61

List of Figures

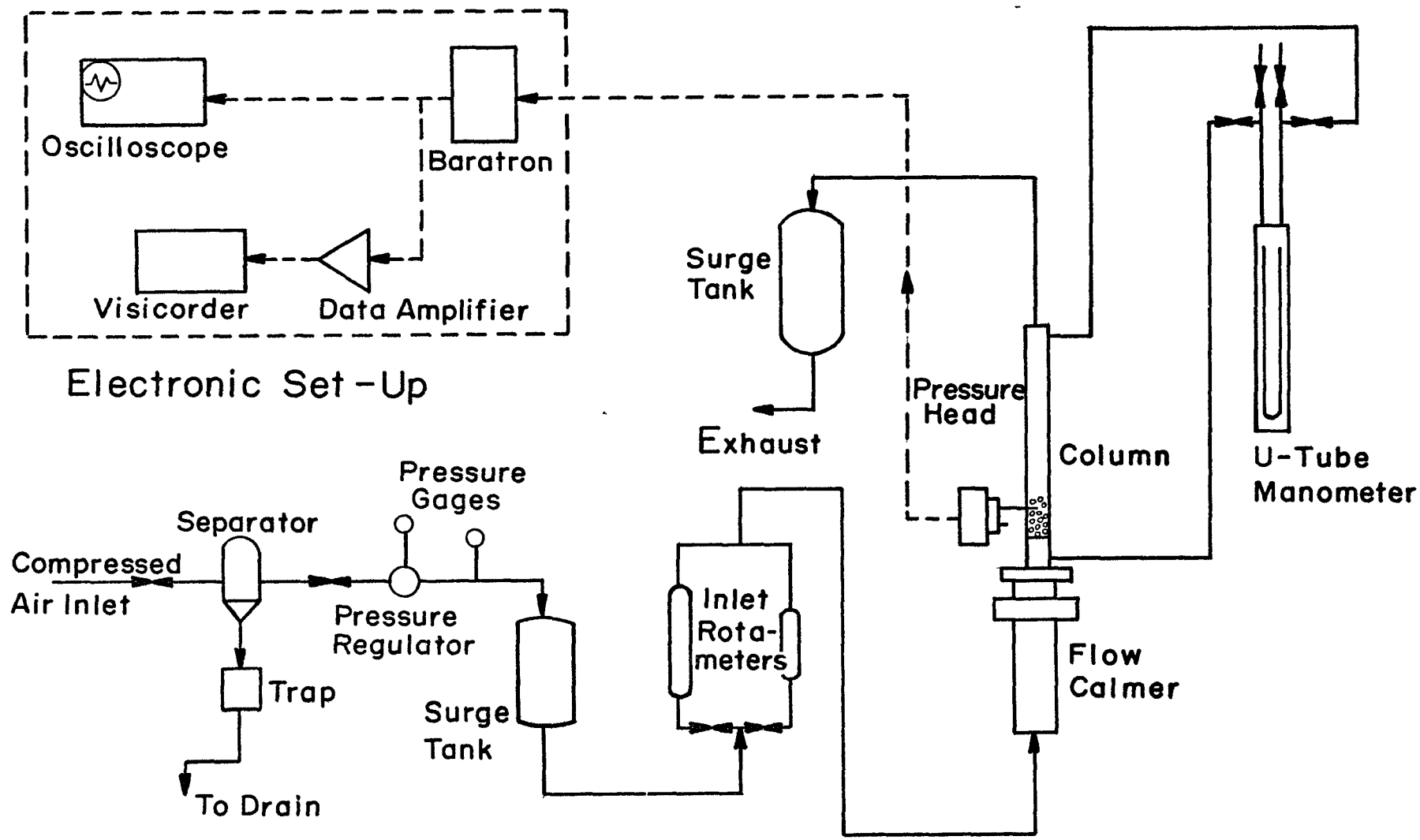

Figure 1

Fig 1

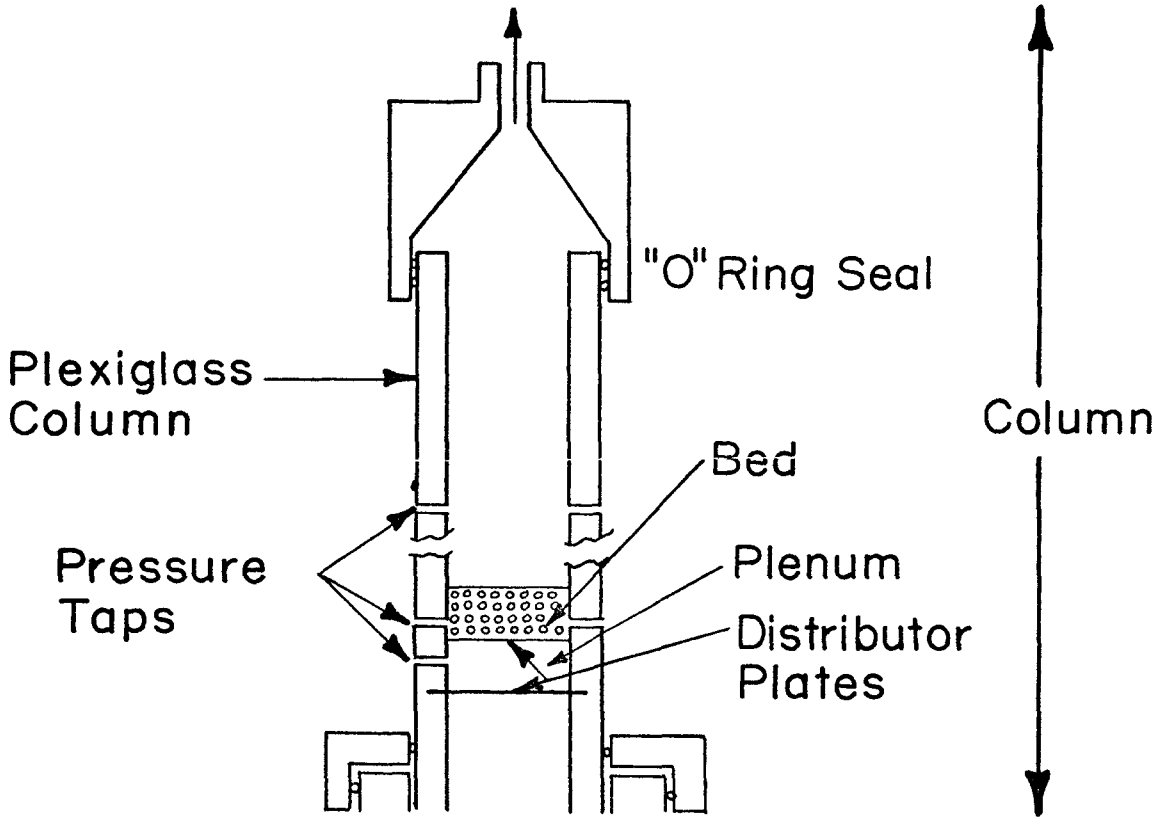

Figure 2

Fig 2

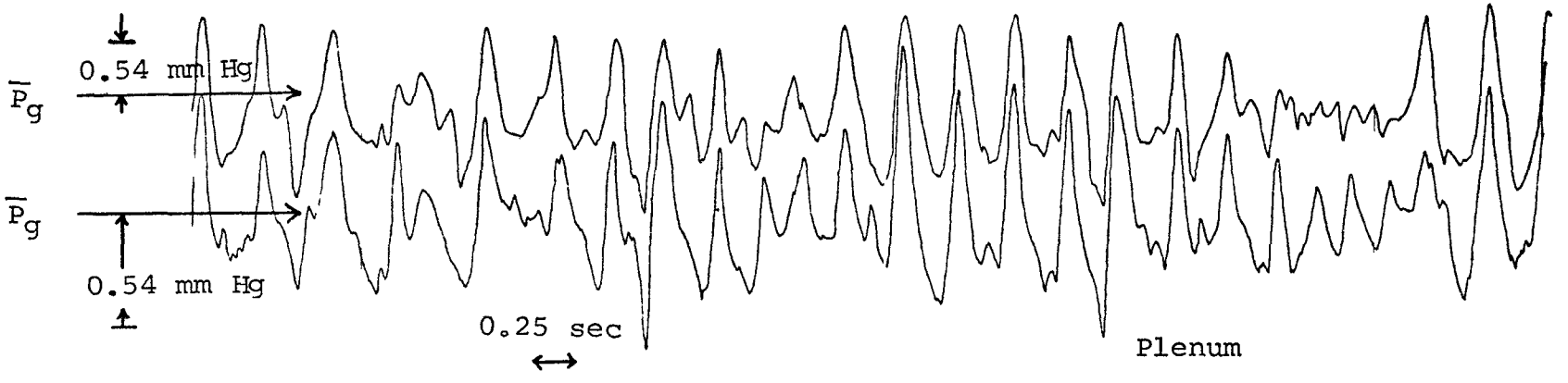
Bed (4.5 in. above distributor plate)
0.54 mm Hg
$\bar{P}_g$
$\bar{P}_g$
0.54 mm Hg
0.25 sec
Plenum

3(a)

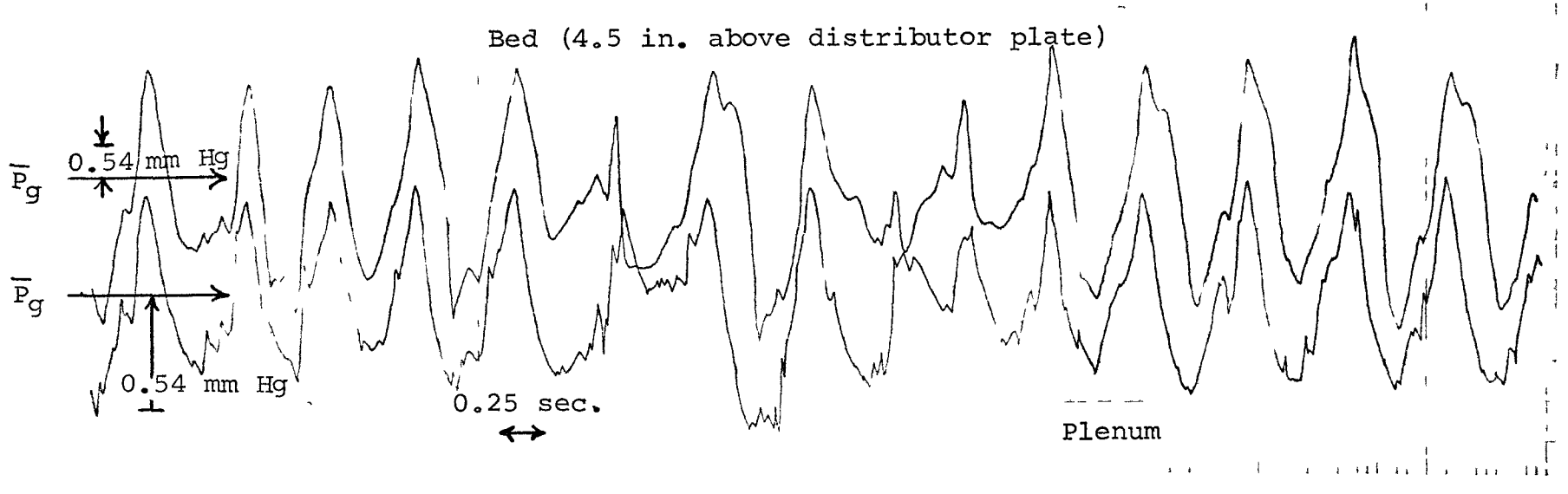
Bed (4.5 in. above distributor plate)
0.54 mm Hg
$\bar{P}_g$
$\bar{P}_g$
0.54 mm Hg
0.25 sec.
Plenum

3(b)

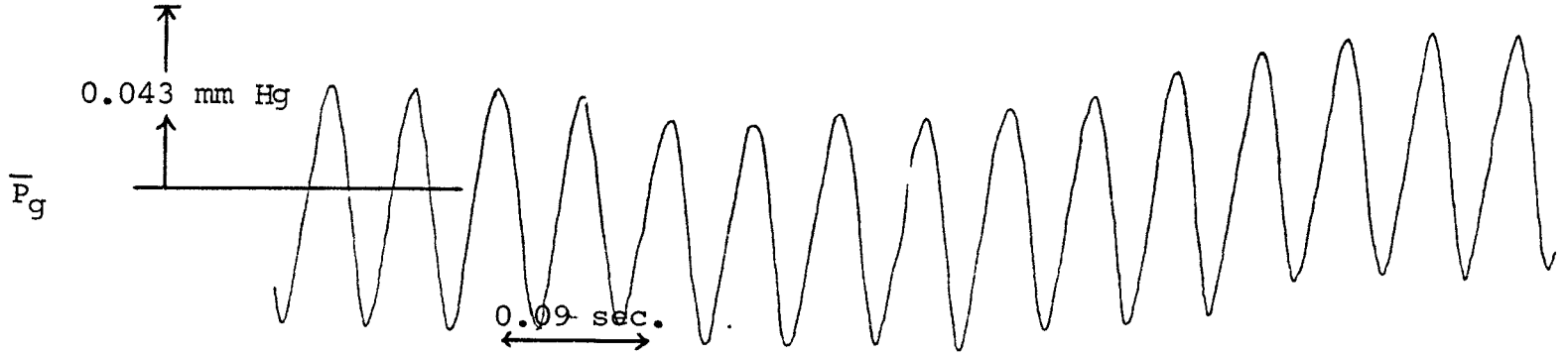
0.043 mm Hg
$\overline{P}_g$
0.09 sec.

4(a)

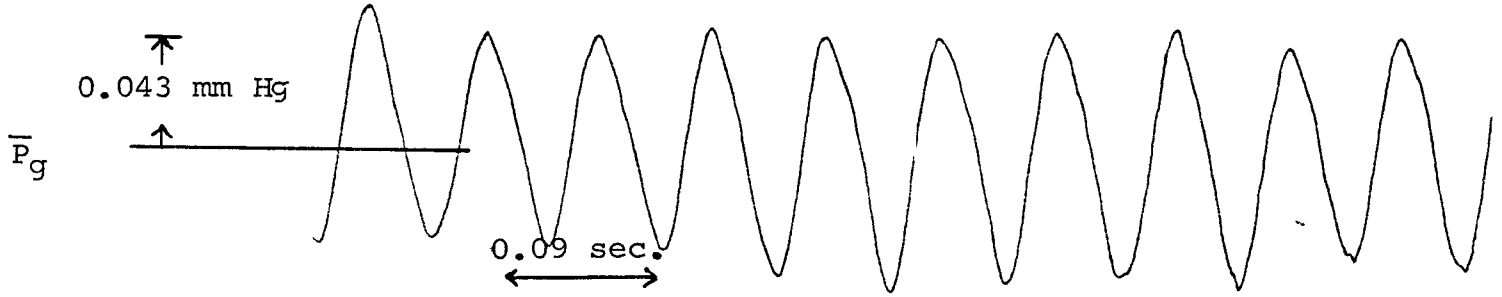
0.043 mm Hg
$\overline{P}_g$
0.09 sec.

4(b)

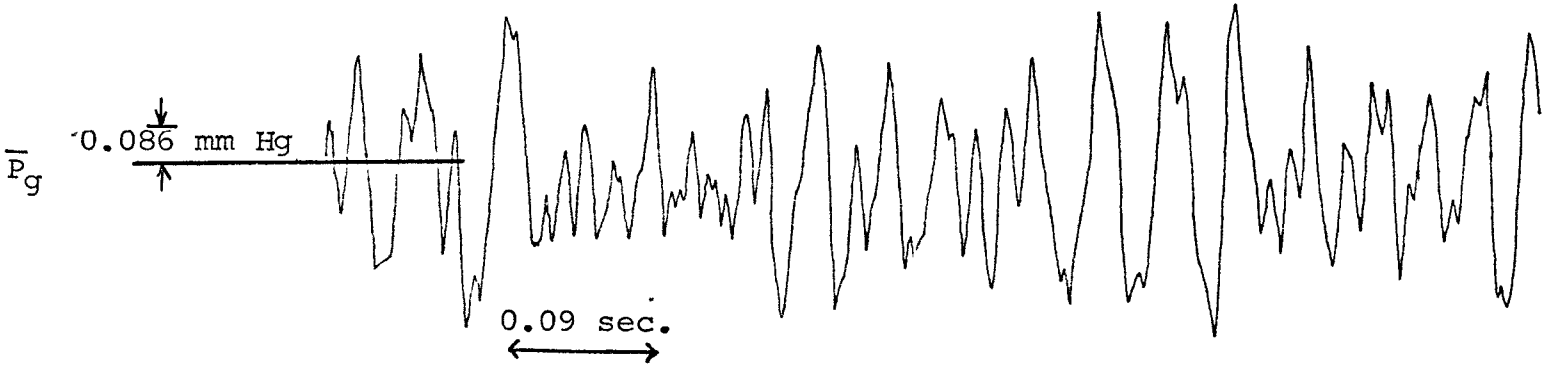
0.086 mm Hg
$\overline{P}_g$
0.09 sec.

4(c)

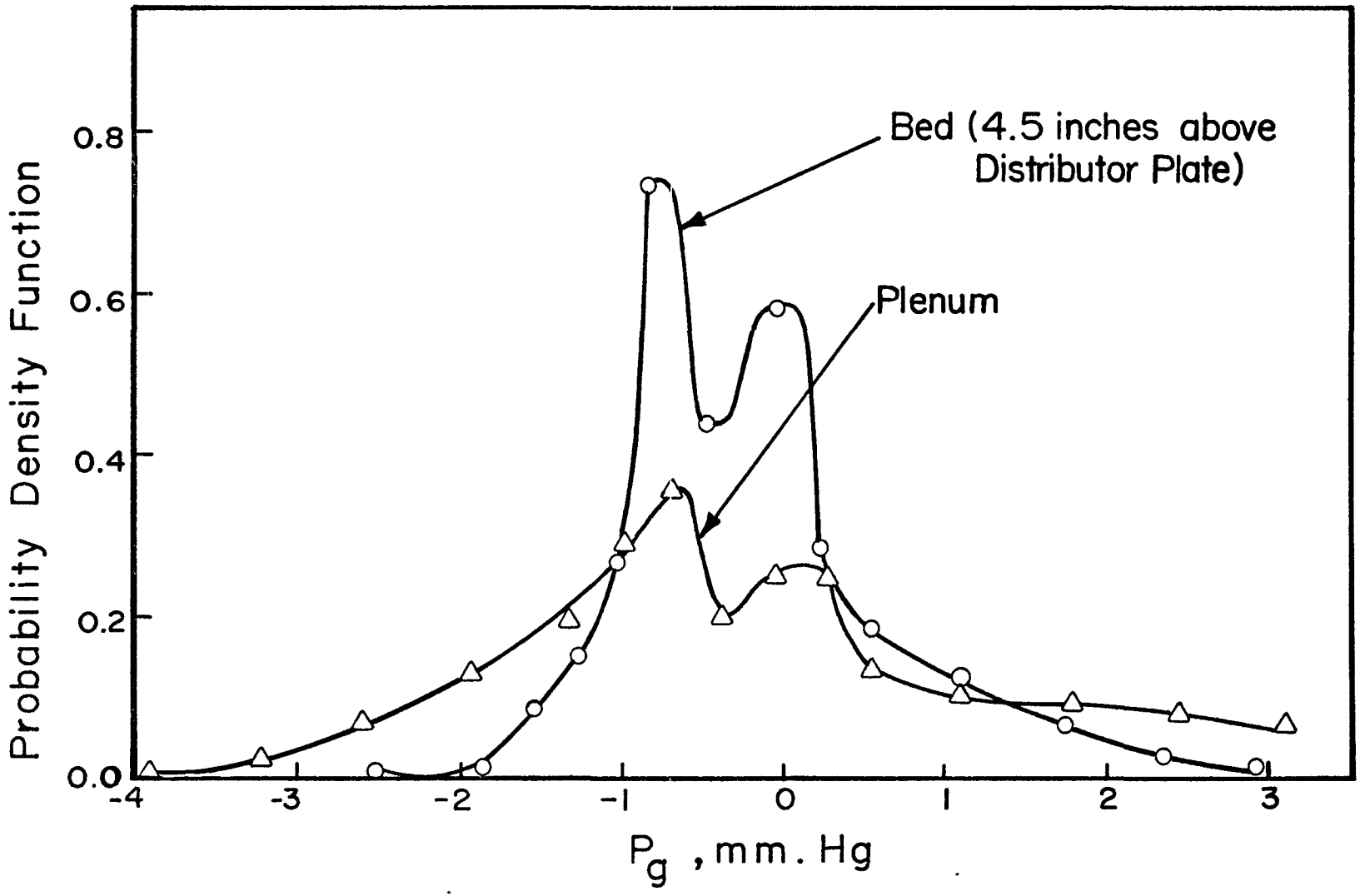

Figure 5

Fig 5

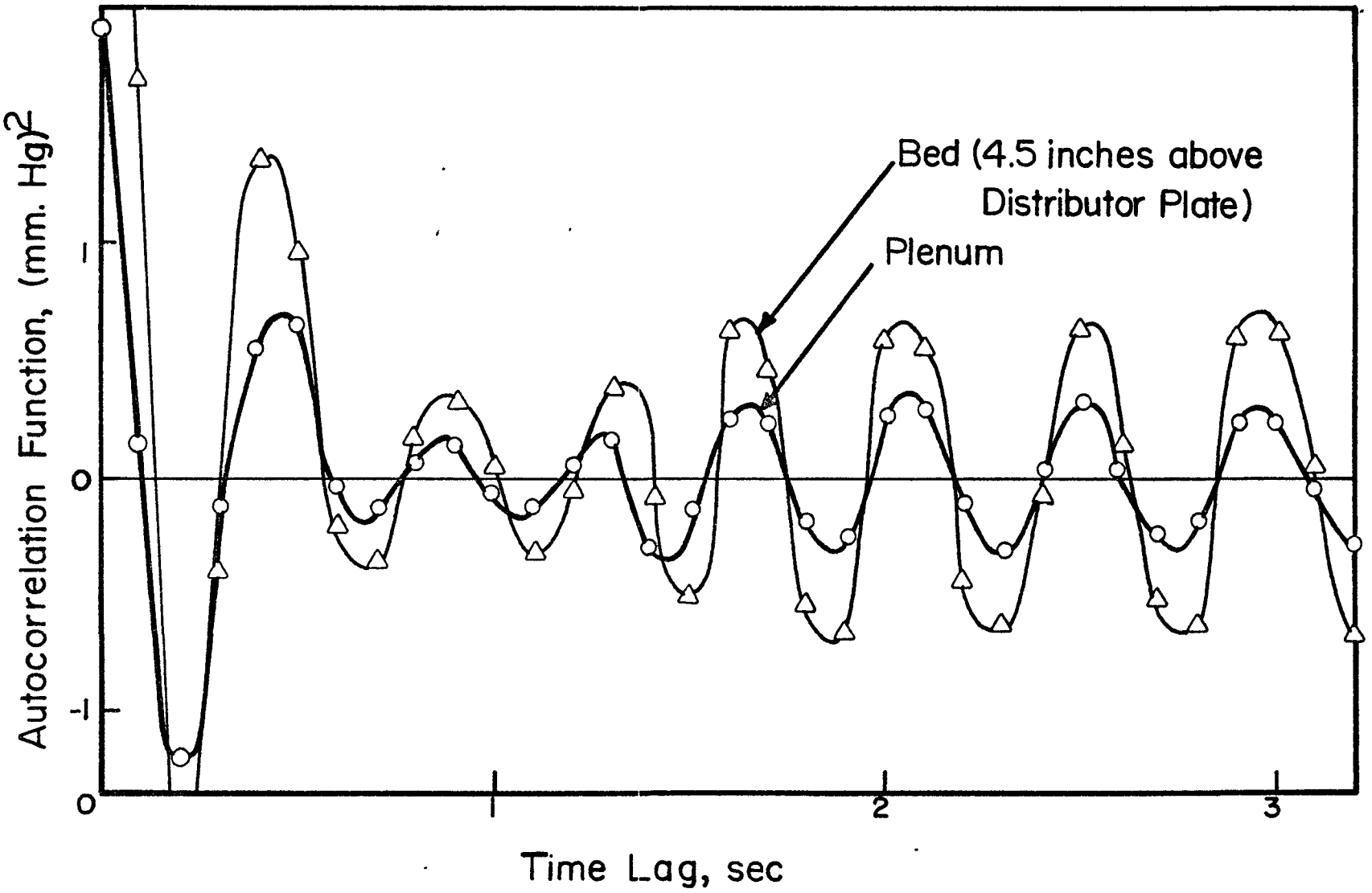
Autocorrelation Function, (mm. Hg)²
1
0
-1
0
2
3
Time Lag, sec
Bed (4.5 inches above Distributor Plate)
Plenum

Fig 6

Fig 6

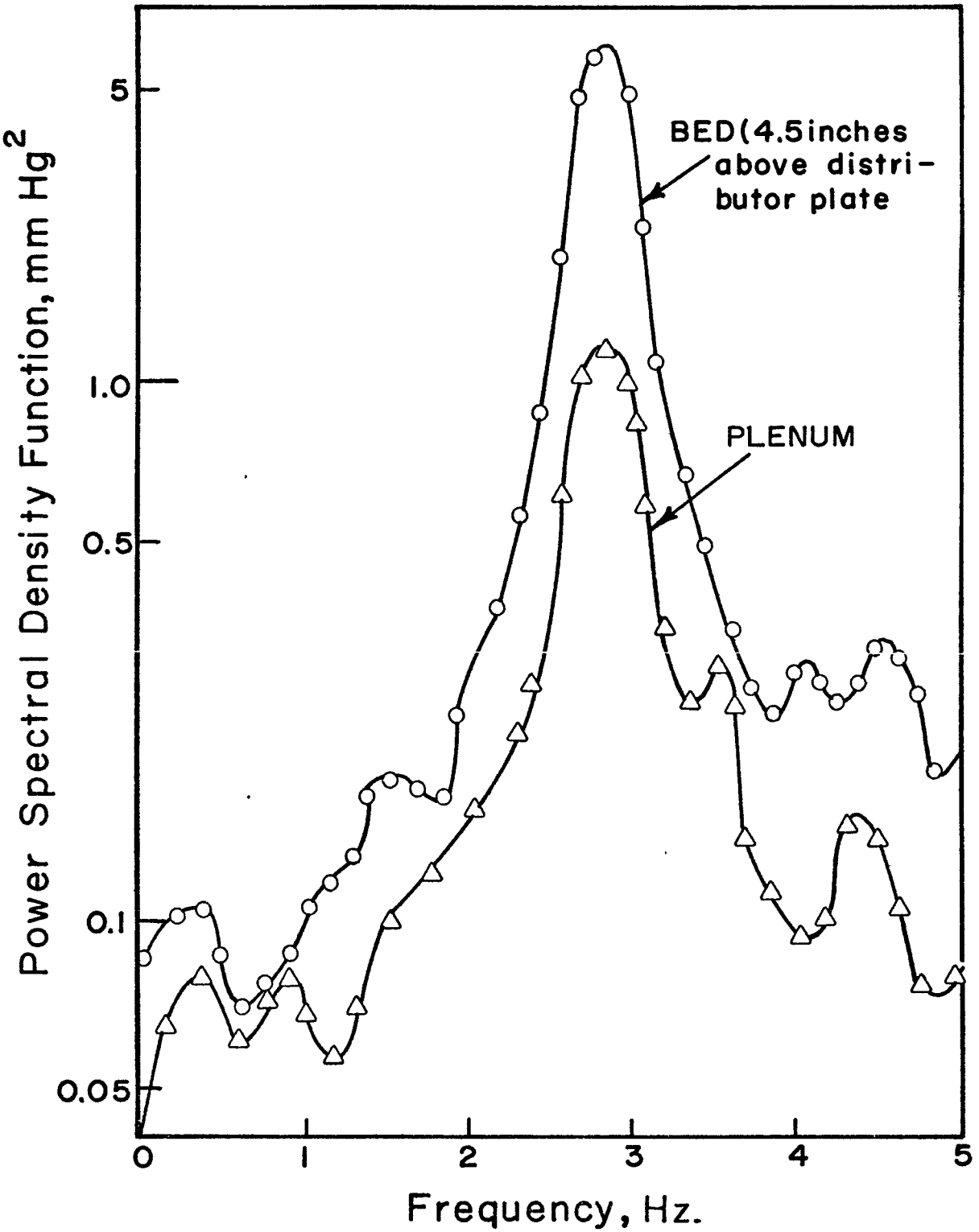

Figure 7

Fig 7

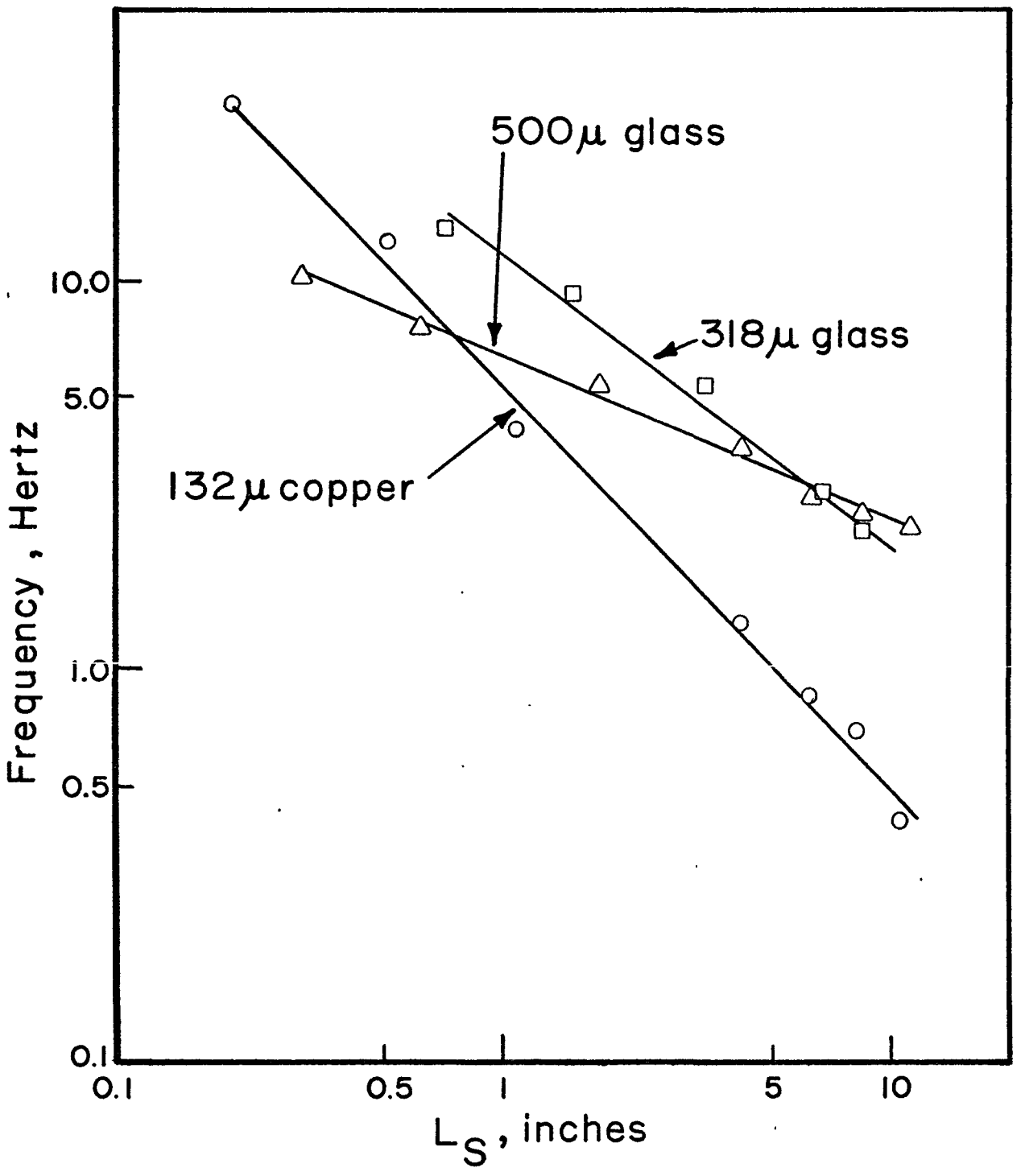

Figure 8

Fig 8

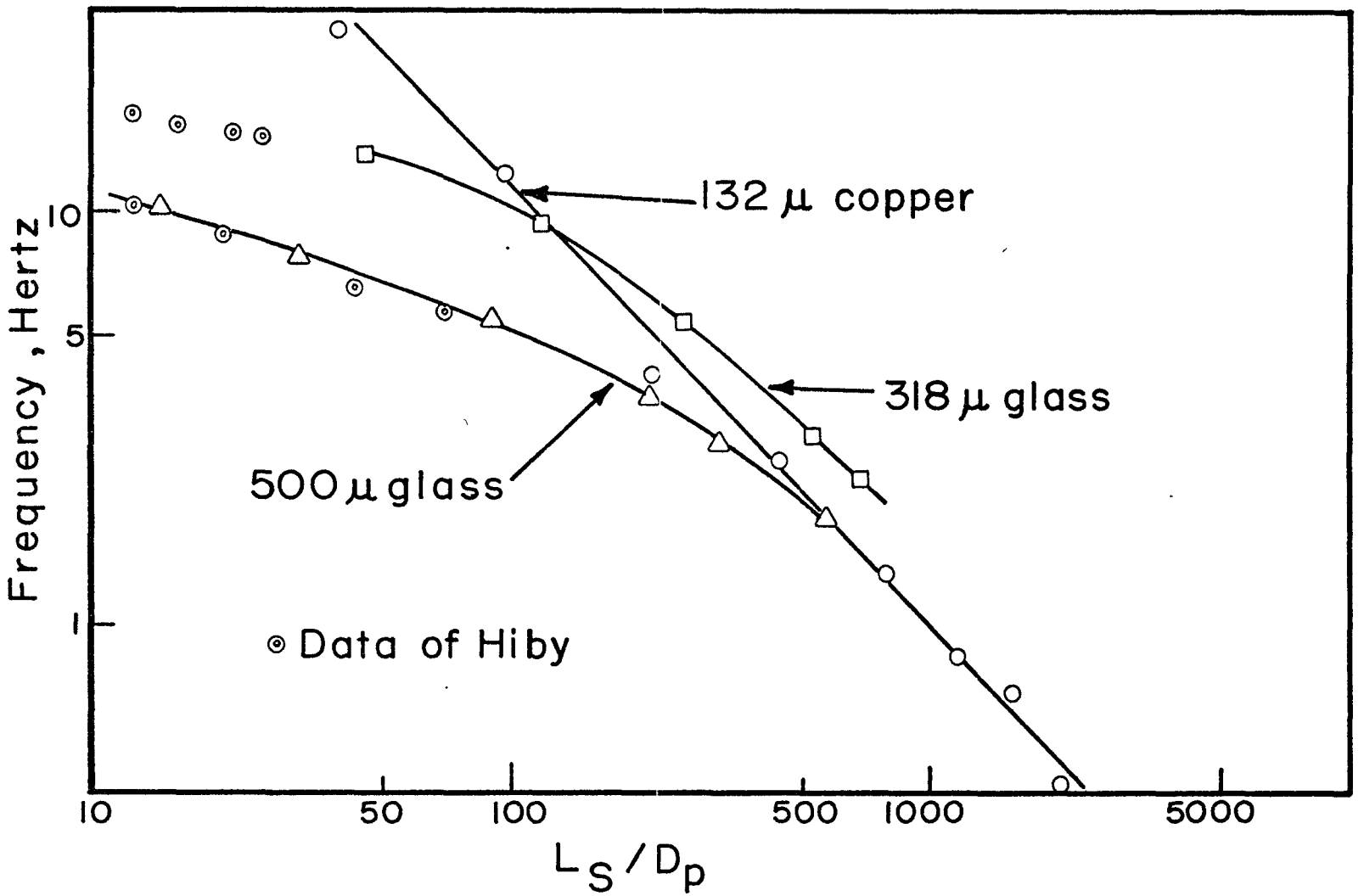

Figure 9

Fig 9

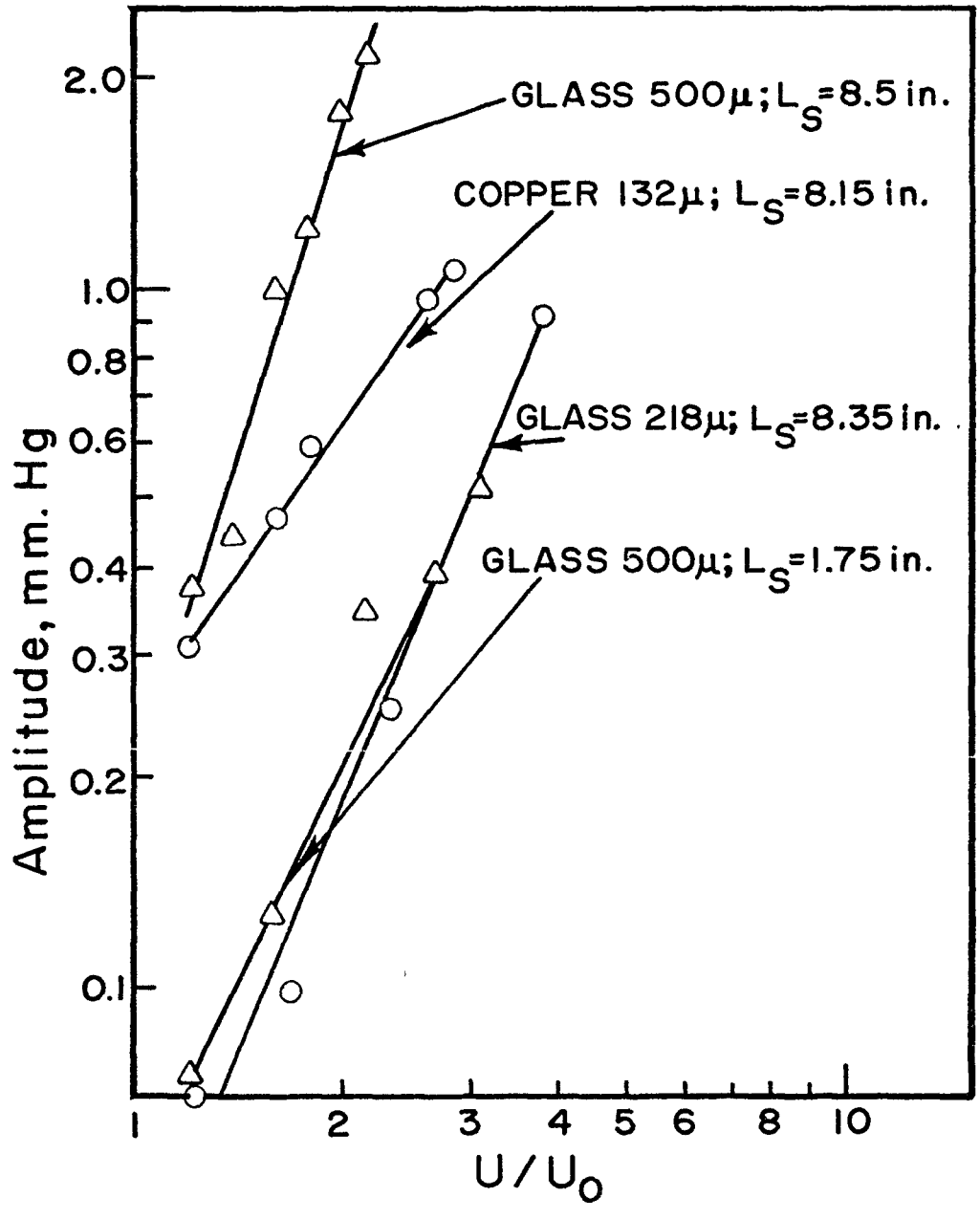

Figure 10

Fig 10

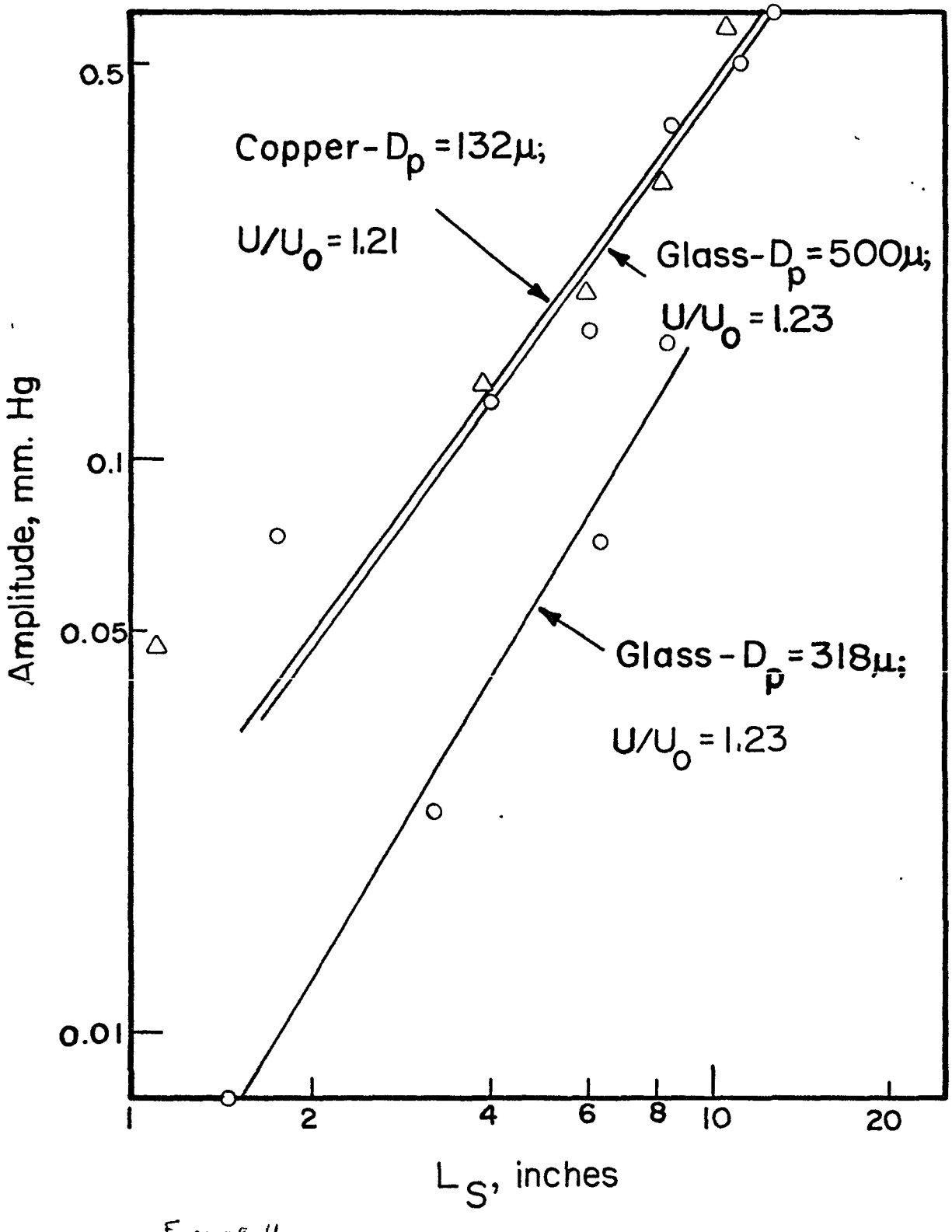

Figure 11

Fig 11

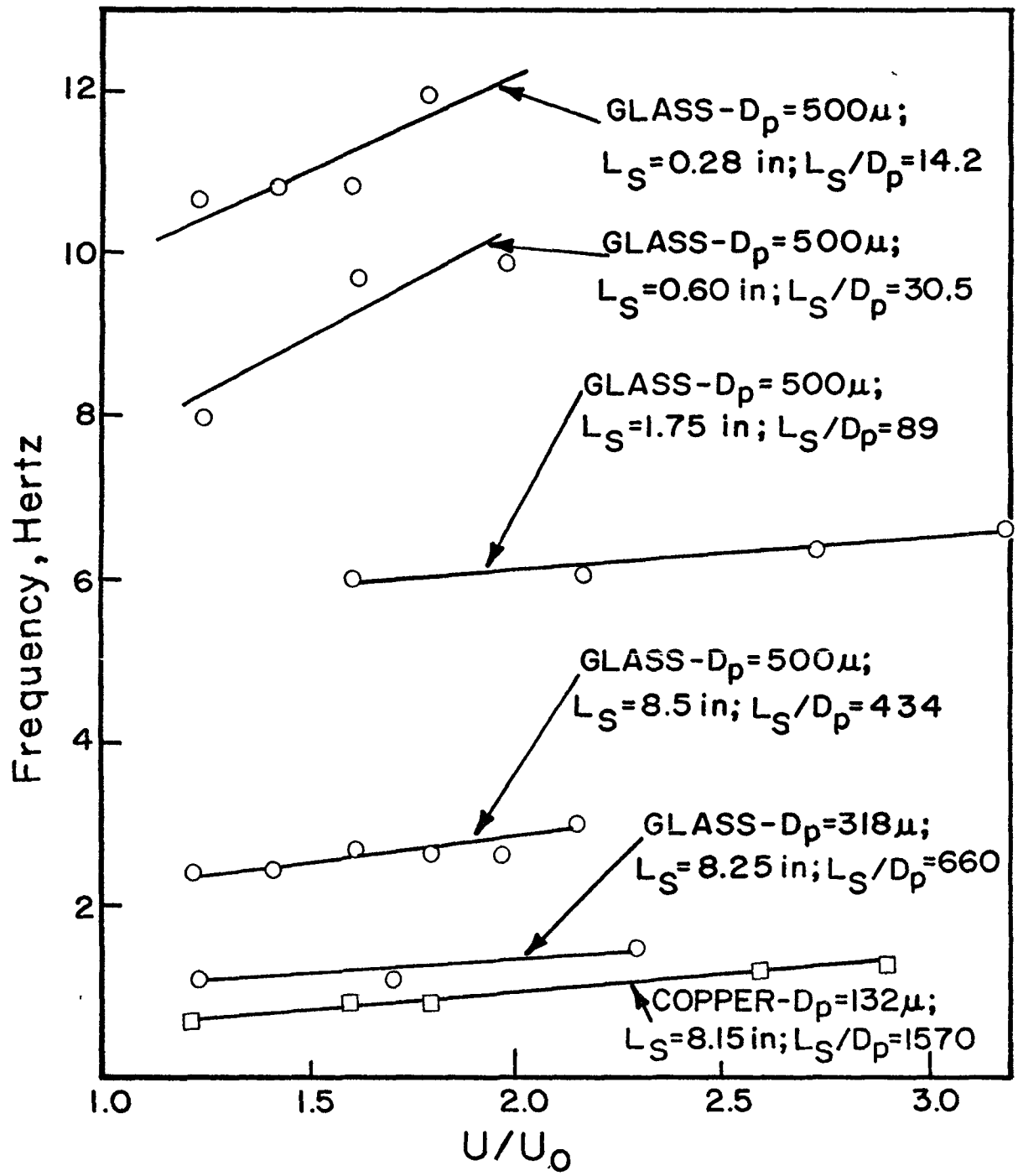

Frequency Hz

Fig 12

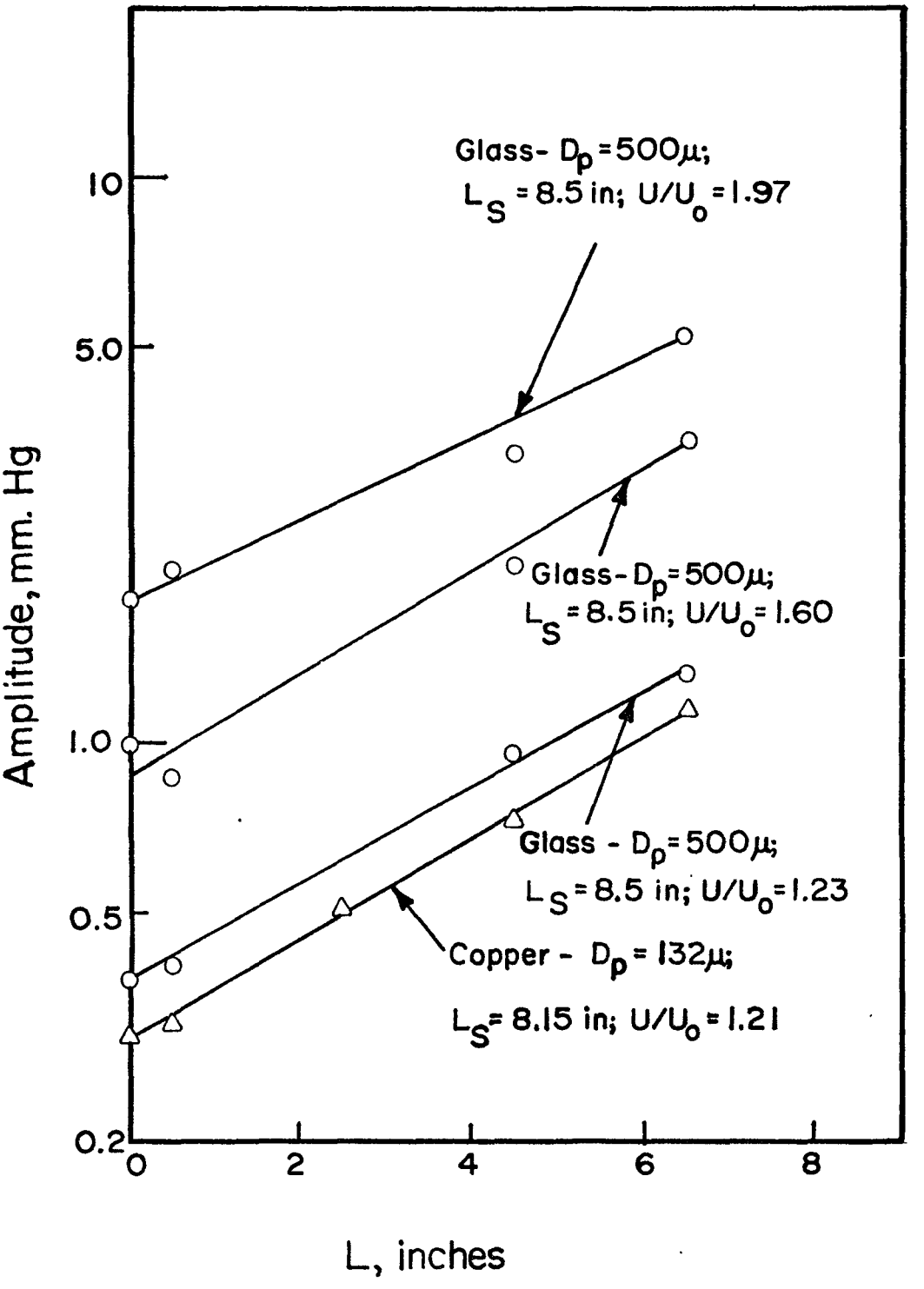
Glass- D_p = 500μ;
L_S = 8.5 in; U/U_o = 1.97
Glass- D_p = 500μ;
L_S = 8.5 in; U/U_o = 1.60
Glass - D_p = 500μ;
L_S = 8.5 in; U/U_o = 1.23
Copper - D_p = 132μ;
L_S = 8.15 in; U/U_o = 1.21
Amplitude, mm. Hg
10
5.0
1.0
0.5
0.2
0
2
4
6
8
L, inches

Fig. 13

Fig 13

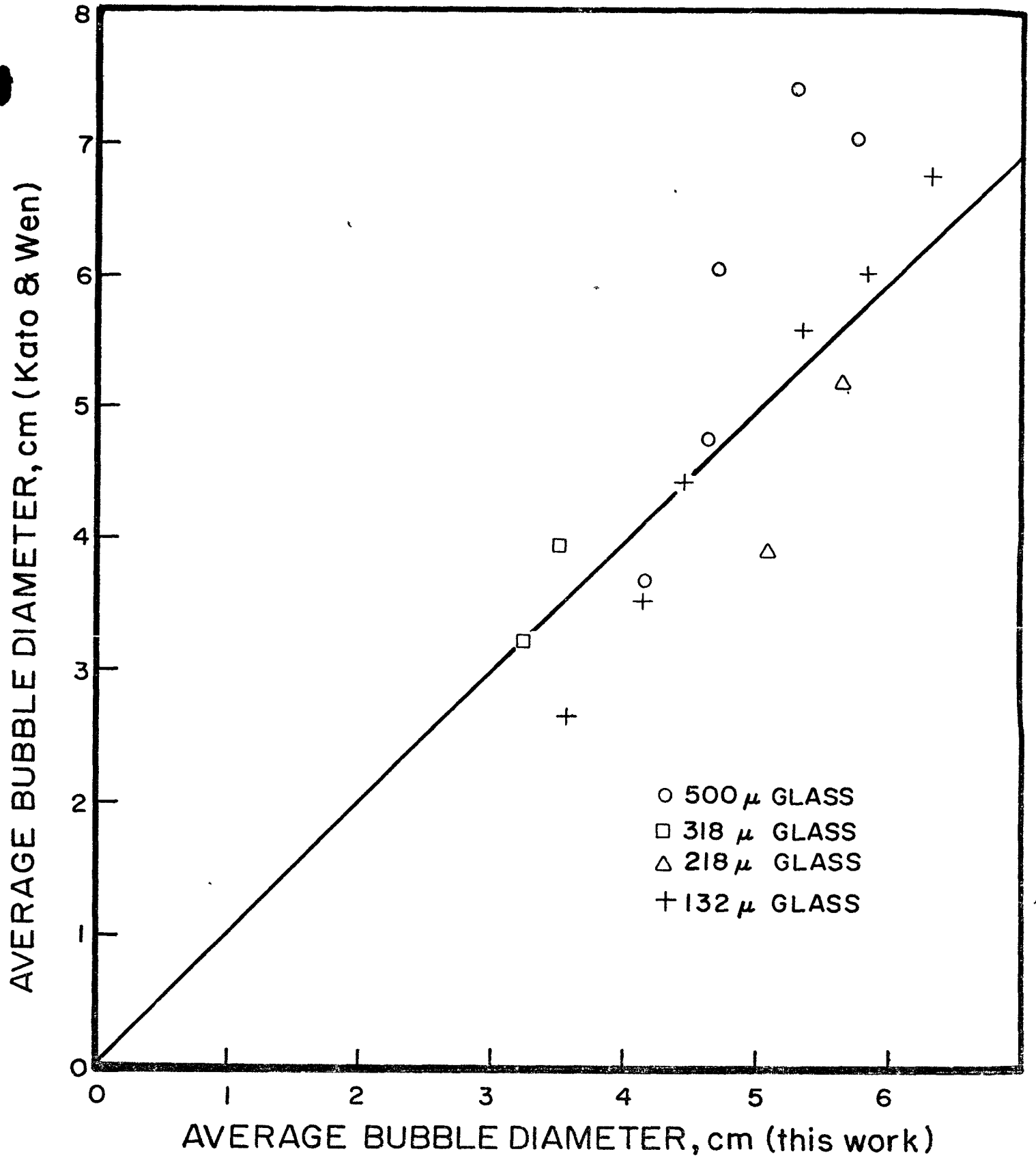
AVERAGE BUBBLE DIAMETER, cm (Kato & Wen)
AVERAGE BUBBLE DIAMETER, cm (this work)
0
1
2
3
4
5
6
7
8
○ 500 μ GLASS
□ 318 μ GLASS
△ 218 μ GLASS
+ 132 μ GLASS

Figure 14